

## Study of Di-electric Constant dependency of $\text{Eu}_2\text{O}_3$ Doped $\text{SrTiO}_3$ Nano-ceramic on Temperature and Frequency

Md. Shafiul Islam\*, Shahnaz Parven, Shujit Chandra Paul and Md. Yusuf Miah

Department of Applied Chemistry & Chemical Engineering, Noakhali Science and Technology University, Bangladesh

\*Corresponding author: Md. Shafiul Islam, Department of Applied Chemistry & Chemical Engineering, Noakhali Science and Technology University, Bangladesh, Tel: +88-01916034310; E-mail: shafiulacce@gmail.com

Received date: Jan 26, 2018; Accepted date: December 12, 2018; Published date: January 01, 2019

Copyright: © 2019 Islam S, et al. This is an open-access article distributed under the terms of the Creative Commons Attribution License, which permits unrestricted use, distribution, and reproduction in any medium, provided the original author and source are credited.

### Abstract

This work aims the temperature and frequency dependence dielectric properties of  $\text{Eu}_2\text{O}_3$  doped  $\text{SrTiO}_3$  (STO) nanoceramic synthesized by solid state reaction method. The crystalline structure, microstructures of  $\text{SrTiO}_3$  polycrystals doped with  $\text{Eu}^{3+}$  at different compositional ratios were studied by XRD and SEM analyses. The X-ray spectra show that the synthesized powder has cubic structure. From the dielectric behavior it was possible to identify that Eu doping produces changes with respect to pure STO. Dielectric constant was found to decrease with increase in frequency and increase with doping content and sintering temperature.

**Keywords** Capacitance; Densification; Loss factor; Solid reaction; Temperature and frequency

### Introduction

Perovskites types of structure materials are of extensive research interest due to their great properties. The most common example of perovskite is  $\text{SrTiO}_3$  (STO) as described as ideal perovskite structure [1]. STO has drawn attention in solid state physics because of its wide range of interesting physical phenomena [2], such as high dielectric constant [3], ferroelectricity [2, 4-6] etc.

Usually STO shows its best dielectric properties at low temperatures. Depending on this, it has become widely usable in devices such as integrated microelectronics and in memory storage [7-9]. However its dielectric permittivity at RT (300) tends to increases even more on cooling following almost the Curie –Weiss law at a temperature range of between 100K and 240K. This allowed to the low microwave losses of  $\text{SrTiO}_3$ ; turn it in the most attractive material for tuneable microwave electronics devices such as: phase shifters, filters, delay lines, tuneable oscillators, etc. Doping is often used to change the dielectric properties of the STO [10-12]. A small number of impurity ions can change the properties of this Perovskite type of structure material [13-15]. At temperatures as low as 1K,  $\text{SrTiO}_3$  may exhibit superconductivity when doped e.g. with Nb, La, Ta or oxygen vacancies.

During the past few years, rare earth materials have been giving satisfactory accomplishment in the ceramic industry [16-17]. Till now only small fraction of the rare earth materials have been consumed for the production of ceramic materials. But the role of the rare earth materials in composite properties is not clear and hence is important to be further explored [18-20].

Europium oxide ( $\text{Eu}_2\text{O}_3$ ) is used as a dopant in some types of glass in lasers and other optoelectronic devices. It is widely used as a redphosphor in television sets and fluorescent lamps, and as an activator for yttrium-based phosphors [21-22]. A recent application of europium is in quantum memory chips which can reliably store information for days at a time; these could allow sensitive quantum

data to be stored to a hard disk-like device and shipped around the country [23].

A number of methods have been developed for the doping of STO, such as solid state reaction, co-precipitation, sol-gel process, hydrothermal route, and so on [24]. Among these methods, solid state reaction method is of great interest because of its simplicity and low cost.

The purpose of this work is to study the effects of doping on the STO perovskite with a gradually increasing amount of Europium in an STO matrix at high temperature. Here we report the result of effect of temperature and frequency on the dielectric properties of doped STO through solid state reaction method for useful technological applications.

### Materials and Methods

STO (99.95%)/  $\text{Eu}_2\text{O}_3$  (99.9 9%) samples with  $x=0.01, 0.02, 0.03, 0.04$  were prepared in ceramic form by solid-state reaction (Table 1). Powders of STO and  $\text{Eu}_2\text{O}_3$  were mixed in stoichiometric proportions thoroughly grinding these powders in an agate mortar and then by ball milling for 24 hours. The resulting powders were dried in oven at  $90^\circ\text{C}$  and calcined at  $850^\circ\text{C}$  for 8 hours with a heating rate of  $10^\circ\text{C}/\text{min}$  using air atmosphere (Figure 1). Polyvinyl alcohol (5% PV A solution) was mixed as binder with the calcined powder to provide some green strength for subsequent handling. Then, it is dried in an oven for 24 hours to evaporate excess PVA. The pellets were prepared using a universal testing machine (UTM) (FS - 300 KN, Testometric, England) at  $25^\circ\text{C}$  with 0.8 gm of powder for every sample to maintain uniformity in thickness. The pellets made by UTM placed in a Z18-14 of Micropyretics Heaters international, high temperature furnace for sintering. Sintering schedule was varied from batch to batch. Here, sintering is carried out at  $1175^\circ\text{C}$ ,  $1200^\circ\text{C}$  and  $1225^\circ\text{C}$  in air atmosphere. However, for every sintering schedule all samples with similar composition were put in the furnace at the same time.

X-ray diffraction experiments were performed after the powders were obtained in order to identify the main crystalline phase of  $\text{SrTiO}_3$

powders recording the diffractogram from  $10^\circ$  to  $90^\circ$  using Bruker's D 8-Discover X-ray diffractometer with  $\text{CuK}\alpha$  radiation.

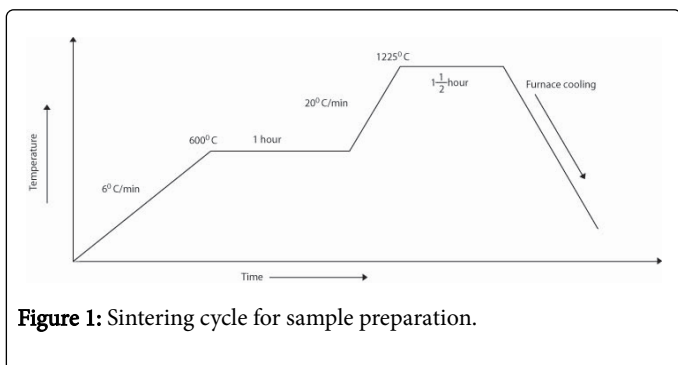


**Figure 1:** Sintering cycle for sample preparation.

The microstructure of the powders was studied by a JEOL FE-SEM-7600F Scanning Electron Microscopy (SEM). Densities of sintered samples were measured by the Archimedes principle method [25]. Dielectric properties of ferrites were carried out by using Keithley Electrometer and Hewlett Packart Impedance Analyzer (WAYNE KERR 6500B). For dielectric measurements, the pellet shaped samples were prepared. Later on the samples were well polished to remove any roughness and the surfaces of each pellet were coated with silver paste as contact material. Dielectric measurements have been done as a function of frequency in the range of 20 Hz to 120 MHz at room Temperature.

S/N	Sample Name	$\text{SrTiO}_3$ (Wt. in gm.)	$\text{Eu}_2\text{O}_3$ (Wt. in gm.)
1	Sample 1	100	1
2	Sample 2	100	2
3	Sample 3	100	3
4	Sample 4	100	4

**Table 1:** Sample Preparation composition.

## Results and Discussion

### Characterization

SEM images of  $\text{Eu}^{3+}$  doped STO samples are illustrated in Figure 2(a)–2(f), respectively. All of them exhibited individual and coalesced grains with irregular shape. Our results are in agreement with other reports where authors showed that the coalescence of grains is favored with a successive increase of the  $\text{Eu}^{3+}$  content [26].

### XRD

From the above images, by comparing with the standard of  $\text{SrTiO}_3$  and  $\text{Eu}_2\text{O}_3$ , it has been cleared that, the X-ray diffraction pattern of all samples are stable in all sintering temperature because of lowest amount of doping. From the XRD data, it can be explained that with changing sintering temperature little difference is found. The intensity is found lower with increasing sintering temperature although no phase shifting has been exhibited at all among them and also with comprise to the standard value. No new phase has been found from the XRD data which ensure the purity of the sample (Figure 3) [27]

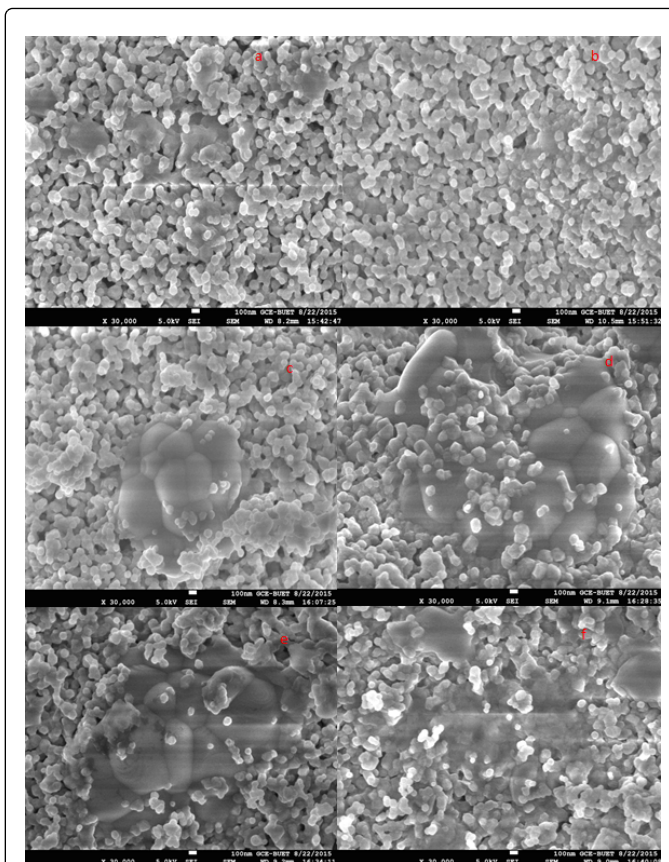


**Figure 2:** SEM Image of a) sample 2 at  $1175^\circ\text{C}$  b) sample 3 at  $1175^\circ\text{C}$  c) sample 2 at  $1200^\circ\text{C}$  d) sample 1 at  $1225^\circ\text{C}$  e) sample 3  $1225^\circ\text{C}$  and f) sample 4 at  $1225^\circ\text{C}$ .

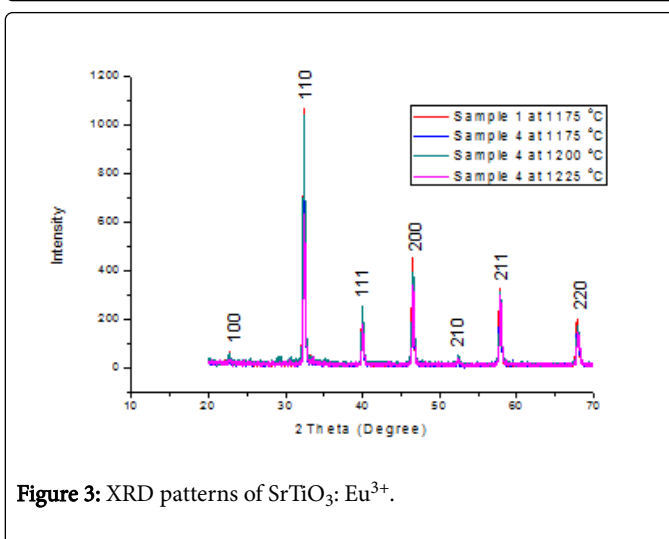


**Figure 3:** XRD patterns of  $\text{SrTiO}_3: \text{Eu}^{3+}$ .

### Densification

Densities of sintered samples were measured by the Archimedes principle method and Figure 4 depicts the percentage of densification of the samples as a function doping content and sintering temperature. From this figure it is clear that with the increase of doping amount and

as well as sintering temperature the percentage of densification increases and then decreases for the maximum doping. The reasons for decreasing densification at higher doping and temperature may be because of reduction in the rate of diffusion mechanisms due to increasing the liquid layer thickness (Figure 2). Differently, due to the increased amount of liquid content, the capillary force between particles decreases resulting in the deceleration densification during sintering [28].

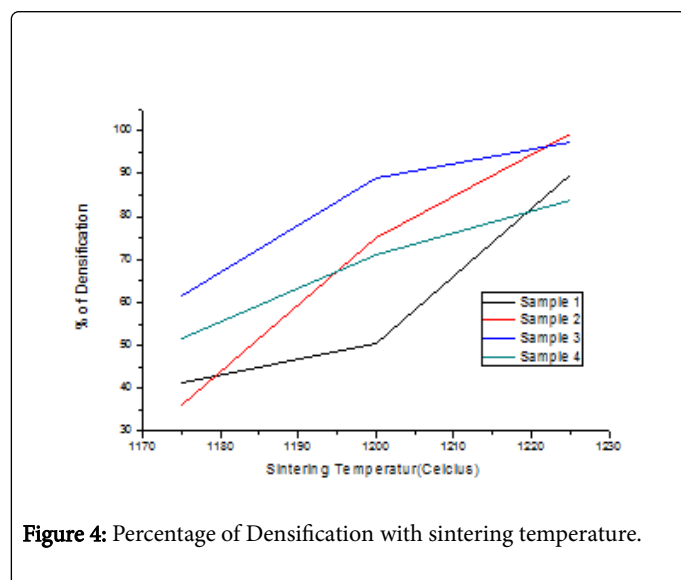


Figure 4: Percentage of Densification with sintering temperature.

### Dielectric constant

Following Figures shows (Figures 5-7) the variation of the dielectric constant with frequency at room temperature for  $\text{Eu}_2\text{O}_3$  doped with 1 gm, 2 gm, 3 gm and 4 gm in 100 gm  $\text{SrTiO}_3$  sample sintered at 1175°C, 1200°C and 1225°C for 1.30 hour.

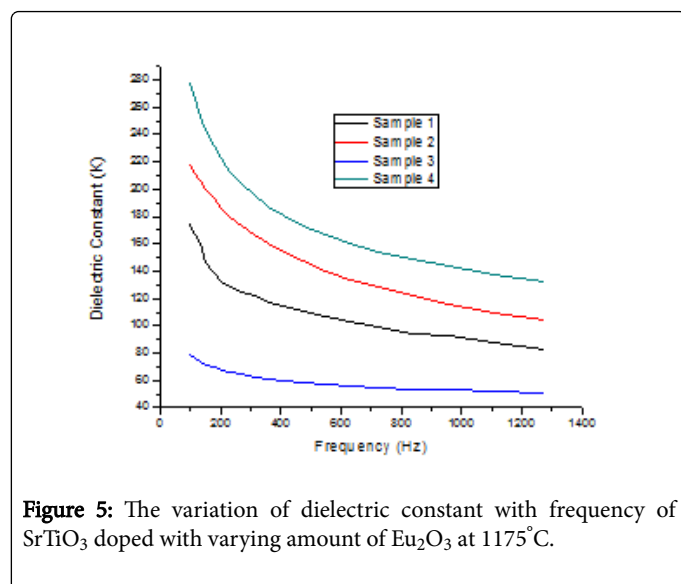


Figure 5: The variation of dielectric constant with frequency of  $\text{SrTiO}_3$  doped with varying amount of  $\text{Eu}_2\text{O}_3$  at 1175°C.

From the two figures (Figures 5-6) it is shown that, with rising frequency the dielectric constant decreases. Dielectric constant of the samples is high at lower frequencies, decreases with increase of frequency by approaching approximately a more or less constant value.

Usually the dielectric constant ( $\epsilon$ ) decreases with the increase in frequency due to decrease in polarization. Polarization of a dielectric material depends on dipolar, electronic, ionic and interfacial polarizations as a sum. Generally at low frequency all types of polarizations respond easily to the time varying electric field but with the increase in frequency, different polarization contributions get weakened, resulting in the decrease of net polarization which leads to the decrease in the value of  $\epsilon$  [29].

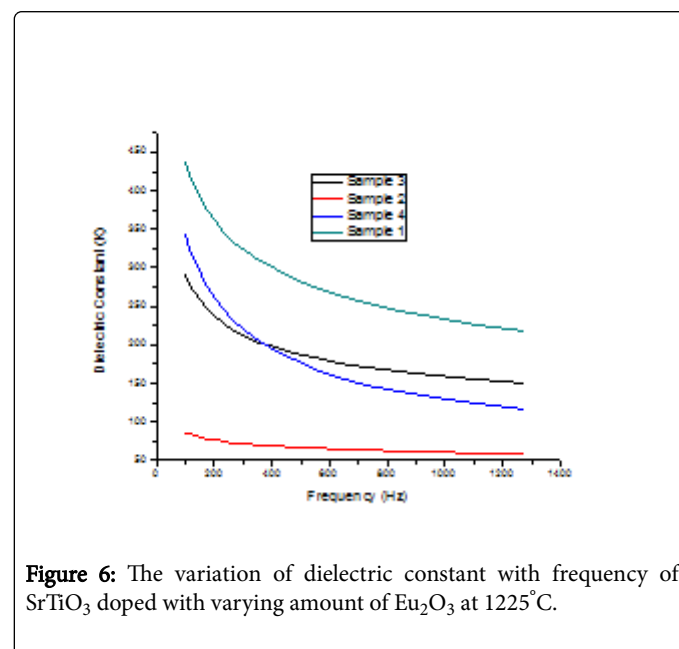
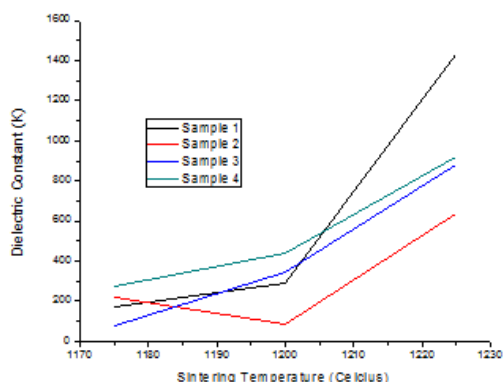


Figure 6: The variation of dielectric constant with frequency of  $\text{SrTiO}_3$  doped with varying amount of  $\text{Eu}_2\text{O}_3$  at 1225°C.

The decrease in dielectric constant at higher frequency can also be explained by assuming that crystalline solid is composed of well conducting grain separated by poorly conducting grain boundaries. The electron through the grain reaches the grain boundary by means of hopping. When the grain boundary is high enough, electrons pile up at the grain boundaries and produce polarization. Thus if the probability of electron reaching the grain boundary decreases, the polarization is also decreases as well. This in turn decreases the dielectric constant [30-31].

From the Figure 7, it can be seen that the highest amount of dielectric constant is obtained for 1gm  $\text{Eu}_2\text{O}_3$  doped  $\text{SrTiO}_3$  sintered at 1225°C. The dielectric constant increases with rising sintering temperature. Here dielectric constant slightly declined for 2 gm  $\text{Eu}_2\text{O}_3$  doped  $\text{SrTiO}_3$ . With sintering, dielectric constant rises due to grain growth and coarsening falling gradually with rising temperature above 1175°C. The dielectric constant increases with increasing temperature for all the composition. The presence of  $\text{Eu}_2\text{O}_3$  creates crystal agglomerate that allows mass transfer between the grains (Figure 1) leading to a more densified microstructure as the temperature is increased (Figure 2). The increase in density causes an increase in Dielectric constant [32-33]. The raise in dielectric constant may also be attributed to the mobile charge carriers related to oxygen vacancies [34]. In addition, agglomerations of powders become a resistant for ions to polarize between grains and grain boundaries indicating greater the agglomeration higher the density and higher the Dielectric constant [35].



**Figure 7:** The variation of dielectric constant with Sintering Temperature of  $\text{SrTiO}_3$  with varying amount of  $\text{Eu}_2\text{O}_3$  at frequency 100 Hz.

During doping  $\text{SrTiO}_3$  with  $\text{Eu}_2\text{O}_3$  the crystal agglomeration is highest for lowest amount of doping (1 gm  $\text{Eu}_2\text{O}_3$ ) which results in highest dielectric constant as compared to other compositions; that means highest amount of doping has lowest densification and hence lowest Dielectric constant value.

### Loss Factor and Capacitance Analysis

Figure 8 shows the variation of loss factor with different sintering temperature at 59.2 MHz. The decrease of  $\tan \delta$  with the increase in frequency can be explained by Debye formula [36]. This formula states that, at lower frequencies there is an inverse relation between  $\tan \delta$  and frequency explaining the decrease in  $\tan \delta$  with frequency. The capacitance is also found to increase with sintering temperature for all composition (Figure 9).

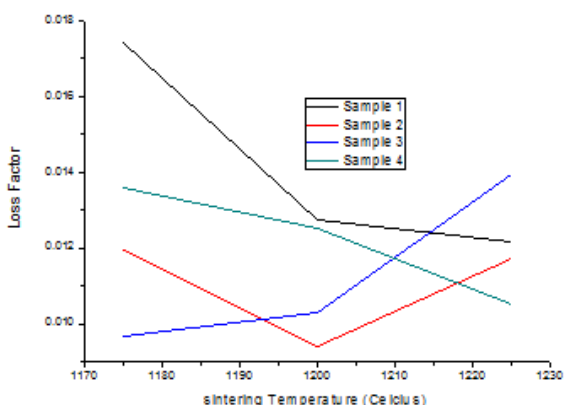


**Figure 8:** Temperature dependent conductance of  $\text{SrTiO}_3$  with varying amount of  $\text{Eu}_2\text{O}_3$  at frequency 59.2 MHz.

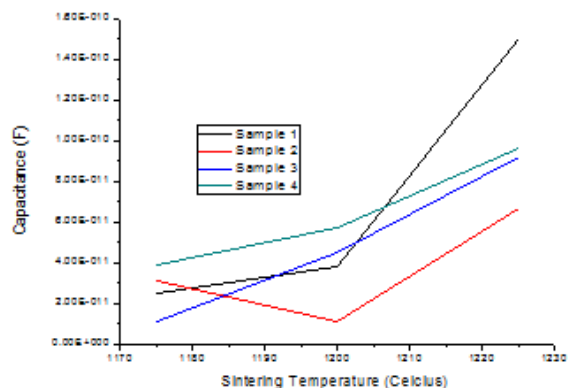


**Figure 9:** The variation of capacitance with composition of  $\text{SrTiO}_3$  with varying amount of  $\text{Eu}_2\text{O}_3$  at frequency 120 MHz.

### Conclusion

The samples of  $\text{EuSrTiO}_3$  composite with different varying composition has been Synthesized successfully by Solid State Reaction route. From the XRD analysis confirmed that all samples has single phase cubic structure for different varying composition and the ascent of any other phases ensures the purity of composite as well. From the density measurement confirmed that the density of the specimens was increased with the sintering temperature and increased doping content. From the dielectric measurement confirmed that, the dielectric constant was increased with decreasing frequency and showed highest dielectric constant for 0.1 gm of  $\text{Eu}_2\text{O}_3$  doped the specimen sintered at  $1225^\circ\text{C}$ .

### Acknowledgement

We are grateful to BCSIR, Bangladesh for their support for successful completion of the various experiments.

### References

1. Mitchell RH (2002) Perovskites : modern and ancient, Almaz Press Inc., Thunder Bay 7: 96.
2. Haeni JH, Irvin P, Chang W, Uecker R, Reiche P, et al. (2004) Room-temperature ferroelectricity in strained  $\text{SrTiO}_3$ . Nature 430: 758-761.
3. Trepakov VA, Kapphan SE, Bednorz JG, Gregora I, Jastrabik L (2004) Dielectric-Related R-Zero-Phonon Emission Line Shift of  $\text{Cr}^{3+}$  in  $\text{SrTiO}_3:\text{Ca}$ . Ferroelectrics 304: 83-86.
4. Garg A, Snedden A, Lightfoot P, Scott JE, Hu X, et al. (2004) Investigation of structural and ferroelectric properties of pulsed-laser-ablated epitaxial Nd-doped bismuth titanate films. J Appl Phys 96: 3408.
5. Samantaray CB, Goswami MLN, Bhattacharya D, Ray SK, Acharya HN (2004) Photoluminescence properties of  $\text{Eu}^{3+}$ -doped barium strontium titanate (Ba, Sr)  $\text{TiO}_3$  ceramics. Mat Lett 58: 2299.
6. Duran A, Martinez E, Diaz JA, J Siqueiros JM (2005) Ferroelectricity at room temperature in Pr-doped  $\text{SrTiO}_3$ . J Appl Phys 97: 104109.
7. Waser R, Dittmann R, Staikov G, Szot K (2009) Redox-Based Resistive Switching Memories – Nanoionic Mechanisms, Prospects, and Challenges. Adv Mater 21: 2632-2663.
8. Gevorgian S (2009) Ferroelectrics in Microwave Devices Circuits and Systems. Springer 62.

9. Ma ZZ, Li JQ, Tian ZM, Qiu Y, Yuan SL (2012) Improved multiferroic properties of La-doped 0.6BiFeO<sub>3</sub>–0.4SrTiO<sub>3</sub> solid solution ceramics. *Chin Phys B* 21107503.
10. Bednorz JG, Muller KA (1984) Sr<sub>1-x</sub>CaxTiO<sub>3</sub>: An XY Quantum Ferroelectric with Transition to Randomness. *Phys Rev Lett* 52: 2289.
11. Ang C, Yu Z, Hemberger J, Lunkenheimer P, Loidl A (1999) Dielectric relaxation modes in bismuth-doped SrTiO<sub>3</sub>: The relaxor behavior. *Phys Rev B* 59: 6665.
12. Bianchi U, Kleemann W, Bednorz JG (1994) Raman scattering of ferroelectric Sr<sub>1-x</sub>CaxTiO<sub>3</sub>, x=0.007. *J Phys: Condens Matt* 6: 1229.
13. Ma JY, Bi CZ, Fang X, Zhao HY, Kamran M, et al. (2007) Optical properties of Nb-doped SrTiO<sub>3</sub> single crystal. *Physica C* 107: 463–465.
14. Gervais F, Servoin JL, Baratoff A, Bednorz JG, Binnig G (1993) Temperature dependence of plasmons in Nb-doped SrTiO<sub>3</sub>. *Phys Rev B* 47: 81-87.
15. Yun JN, Zhang ZY, Yan JF, Deng ZH (2010) *Chin Phys B* 19017101.
16. Corbett, John D (1986) Frank Harold Spedding. Biographical Memoirs National Academy of Sciences (National Academy of Sciences) 80: 106.
17. Caro, Paul (1998) Rare earths 323–325. ISBN 978-84-89784-33-8.
18. Gschneidner KA, Bunzli JC, Pecharsky VK (2005) Handbook on the Physics and Chemistry of Rare Earths.
19. Singhal S, Kaur J, Namgyal T, Sharma R (2012) *Physica B Condens Matt* 407: 1223-1226.
20. Mazen, SA (2000) Tetravalent ions substitution in Cu-ferrite; structure formation and electrical properties. *Mater Chem Phys* 62: 131–138.
21. G. Yoldjian (1985) The use of rare earths in ceramics. *J Less-Common Met* 111:17-22.
22. Baldacim SA, Santos C, Silva OMM, and Silva CRM (2004) Ceramics composites Si<sub>3</sub>N<sub>4</sub>–SiC (w) containing rare earth concentrate (CRE) as sintering aids. *Mater Sci Eng A* 367: 312–316.
23. Inoue M, Otsu H, Kominami H, Inui T (1995) Glycothermal synthesis of rare earth aluminium garnets *J Alloys Compounds* 226: 146–151.
24. Terao R, Tatami J, Meguro T, Komeya K (2002) Fracture behavior of AlN ceramics with rare earth oxides. *J European Ceramic Society* 22: 1051–1059.
25. Xu C, Ai X (2001) Particle dispersed ceramic composite reinforced with rare earth additions. *Int J of Refractory Met Hard Mater* 19: 85–88.
26. Garcia CR, Oliva J, Romero MT, Ochoa-Valiente R, Garcia Trujillo LA (2015) Effect of Eu<sup>3+</sup> Concentration on the Luminescent Properties of SrTiO<sub>3</sub> Phosphors Prepared by Pressure-Assisted Combustion Synthesis. *Adv Mater Sci Engin.*
27. Goncalves RF, Mourac AP, Godinhobc MJ, Longoc E, Machado MAC (2014) Crystal growth and photoluminescence of europium-doped strontium titanate prepared by a microwave hydrothermal method. *Ceramics International* 41: 3549-3554.
28. Janghorban K, Shokrollahi H (2007) Influence of V<sub>2</sub>O<sub>5</sub> addition on the grain growth and magnetic properties of Mn-Zn high permeability ferrites. *J Magn Magn Mater* 308: 238–242.
29. Naceur H, Megriche A, Maaoui ME (2013) Frequency-dependant Dielectric Characteristics and Conductivity Behavior of Sr<sub>1-x</sub>(Na<sub>0.5</sub>Bi<sub>0.5</sub>)<sub>x</sub>Bi<sub>2</sub>Nb<sub>2</sub>O<sub>9</sub> (x = 0.0, 0.2, 0.5, 0.8 and 1.0). *Ceram Orient J Chem* 29:937-944.
30. Venkataraju C, Sathishkumar G, Sivakumar K (2010) Effect of Nickel on the Electrical Properties of Nanostructured MnZn Ferrite. *J Alloys Comp* 498: 203-206.
31. Das T, Das BK, Parashar K, Parashar SKS (2016) Temperature and Frequency Dependence Electrical Properties of Zn<sub>1-x</sub>CaxO Nanoceramic. *Acta Physica Polonica A* 130.
32. Chen H, Yang C, Fu C, Zhao L, Gao Z (2006) The size effect of Ba<sub>0.6</sub>Sr<sub>0.4</sub>TiO<sub>3</sub> thin films on the ferroelectric properties. *Appl Surf Sci* 252: 4171–4177.
33. Xu Q, Zhang XF, Liu HX, Chen W, Chen Min, et al. (2011) Effect of sintering temperature on dielectric properties of Ba<sub>0.6</sub>Sr<sub>0.4</sub>TiO<sub>3</sub>–MgO composite ceramics prepared from fine constituent powders. *Mater Design* 32: 1200–1204.
34. Cheng ZX, Wang XL, Dou SX, Ozawa K, Kimura H (2007) Ferroelectric properties of Bi<sub>3.25</sub>Sm<sub>0.75</sub>V<sub>0.02</sub>T<sub>2.98</sub>O<sub>12</sub> thin film at elevated temperature. *Appl Phys Lett* 90: 222902.
35. Yan LC, Hassan J, Hashim M (2011) Effect of sintering temperatures on the microstructure and dielectric properties of SrTiO<sub>3</sub>. *W Appl Sci J* 15: 1614–1618.
36. Birey H (1978) Dielectric properties of aluminum oxide films. *J Appl Phy* 49: 2898.